PROTEINS WILEY

GABA receptor associated protein changes the electrostatic environment around the GABA type A receptor

Benedict W. J. Irwin[1] | Clara C. Wanjura[1] | Daniel Molnar[1] | Michael J. Rutter[1] |
Michael C. Payne[1] | P.-L. Chau[2] ⓘ

[1]Theory of Condensed Matter Group,
Cavendish Laboratory, Department of Physics,
University of Cambridge, Cambridge, UK

[2]Bioinformatique Structurale, Institut Pasteur,
CNRS URA 3528, CB3I CNRS USR 3756,
Paris, France

Correspondence
P.-L. Chau, Bioinformatique Structurale,
Institut Pasteur, CNRS URA 3528, CB3I CNRS
USR 3756, 75724 Paris, France.
Email: pc104@pasteur.fr

Funding information
Science and Technology Facilities Council;
Engineering and Physical Sciences Research
Council, Grant/Award Number: EP/
P020259/1; INCEPTION, Grant/Award
Number: ANR-16-CONV-0005

Abstract

We have performed fully atomistic molecular dynamics simulations of the intracellular domain of a model of the $GABA_A$ receptor with and without the GABA receptor associated protein (GABARAP) bound. We have also calculated the electrostatic potential due to the receptor, in the absence and presence of GABARAP. We find that GABARAP binding changes the electrostatic properties around the $GABA_A$ receptor and could lead to increased conductivity of chloride ions through the receptor. We also find that ion motions that would result in conducting currents are observed nearly twice as often when GABARAP binds. These results are consistent with data from electrophysiological experiments.

KEYWORDS
GABARAP, $GABA_A$ receptor, ionic conductance, electrostatic potential, ligand-gated ion channels

1 | INTRODUCTION

The family of $GABA_A$ receptors is responsible for the majority of fast neuronal inhibition in the mammalian central nervous system, and is a target of general anesthetics, benzodiazepines, barbiturates and neurosteroids. These pentameric proteins belong to the cys-loop family of ligand-gated ion channels that includes the nicotinic acetylcholine, glycine, and $5HT_3$ receptors. The $GABA_A$ receptors are composed of five subunits arranged pseudosymmetrically around the central ion channel.[1] The subunits, of which 19 have thus far been identified, are separated into classes based on their sequence similarity: there are six α-subunits, three β, three γ, three ρ, and single representatives of δ, ϵ, θ, and π.[2] The precise subunit isoform composition of the pentamer defines the recognition and biophysical characteristics of the particular receptor subtype. The most ubiquitous subtype, which accounts for approximately 30% of $GABA_A$ receptors in the mammalian brain,[3]

contains two α_1-, two β_2-, and a single γ_2-subunit.[4] The $GABA_A$ receptors can be divided into three structural domains, the extracellular (EC) domain, the transmembrane (TM) domain, and the intracellular (IC) domain. When GABA binds to the $GABA_A$ receptor, the central ion channel opens to let chloride ions through.[5] This opening is quickly followed by a period of desensitization of the receptor.[6]

$GABA_A$ receptors with a γ-subunit are often associated with the $GABA_A$-receptor associated protein, GABARAP. This protein, first described by Wang et al.,[7] consists of 117 amino acids and has a relative molecular mass of 13 900. Experimental work[7,8] shows that it binds to the intracellular domain of the γ_2-subunit of the $GABA_A$ receptor. Its function is most probably twofold: anchoring the $GABA_A$ receptor to the cytoskeleton, and modulating the function of the receptor. Amino acids near the N-terminal of GABARAP could bind to tubulin,[9] whilst the amino acids nearer the C-terminal bind to the $GABA_A$ receptor.[8] Moreover, Chen et al.[10] showed that GABARAP caused $GABA_A$ receptor clustering, and clustered receptors exhibited lower affinity for GABA (EC_{50} increased from 5.74 ± 1.4 μM to 20.27 ± 3.8 μM), and they

Benedict W. J. Irwin and Clara C. Wanjura have contributed equally to this study.

desensitized less quickly (the desensitisation time constant τ increased from 1 to 2 s). Luu et al.[11] show that GABARAP binding increases the conductance of the GABA$_A$ receptor from below 40 pS to above 50 pS, and the mean opening times from about 2 ms to about 6 ms.

Nevertheless, we still do not know how GABARAP binding changes the conductance of the GABA$_A$ receptor. Previous study by Irwin et al.[12] used experimental structures of the GABARAP and a modeled structure of the intracellular domain of the GABA$_A$ receptor and performed docking, molecular dynamics simulations and inhomogeneous fluid solvation theory calculations to predict the interaction between GABARAP and the GABA$_A$ receptor. We build on this study and use molecular dynamics simulations and electrostatic calculations to elucidate how GABARAP binding could increase the conductance of the GABA$_A$ receptor.

2 | METHODS

2.1 | Molecular coordinates

In this research, we used the coordinates of a GABA$_A$ receptor model from the study of Mokrab et al..[13] This model used, as template, the nicotinic acetylcholine receptor (nAChR) structure from the study of Unwin,[14] where five intracellular helices were resolved (Protein Data Bank code: 2BG9). This is the only structure of the GABA$_A$ receptor, experimental or modeled, that includes part of the intracellular domain. The subunit composition of this receptor is $(\alpha_1)_2(\beta_2)_2\gamma_2$. The intracellular helices are defined to be the following amino acids: α_1-subunit Lys 391–Asp 420, β_2-subunit His 421–Asp 450, γ_2-subunit Asp 413–Asp 442.

For the GABARAP structure, we use dock 54a of structure 15 of the NMR solution structure (PDB code: 1KOT[15]) from previous study.[12] Figure 1 shows the interaction between GABARAP and the

GABA$_A$ receptor intracellular pentahelix viewed from the extracellular space towards the cytoplasm. Figure 2 shows the interaction between GABARAP and the GABA$_A$ receptor intracellular pentahelix from the side, with two amino acids from GABARAP and two amino acids from the pentahelix labeled.

2.2 | Molecular dynamics simulation of GABARAP and intracellular helices

The systems were prepared using the CHARMM-GUI freely available on the web.[16] The molecular dynamics package NAMD 2[17] was used in this study.

We took the pentahelix and immersed it in a solution consisting of 38658 water molecules, 110 K$^+$ ions and 123 Cl$^-$ ions in a periodic rhombohedral box measuring 108.9 Å by 109.0 Å by 108.8 Å which gives an ionic solution of concentration of about 0.15 M. We also took the pentahelix/GABARAP complex and immersed it in a solution consisting of 38024 water molecules, 108 K$^+$ ions and 123 Cl$^-$ ions in a periodic rhombohedral box of the same dimensions which gives an ionic solution of concentration of about 0.15 M. These protein molecules are charged, so unequal numbers of cations and anions are included to render the final systems electrically neutral. In both cases, the protein is at least 10 Å from any part of its image in the next periodic box.

We used the CHARMM potential for all our simulations.[18] Each system was minimized for 10 000 steps with all the protein atoms frozen. Molecular dynamics at 310 K was initialized for 10 000 time-steps of 0.1 fs each, with all main-chain nitrogen atoms frozen. Langevin dynamics was applied; the thermostat was set with a time constant of 1 ps^{-1}, and the barostat set with a piston decay time of 10 ps and a piston period of 20 ps. The van der Waals cut-off was 12 Å, and Ewald summation was used for the electrostatic interactions arising from the cell's periodic images. The time-step was
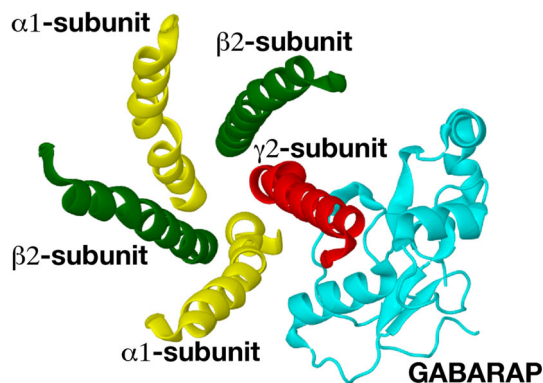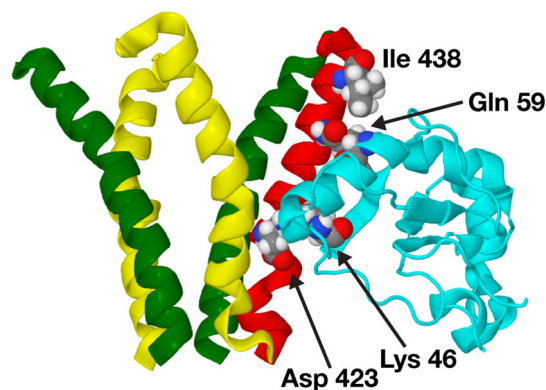

FIGURE 1 Model of the GABA$_A$ receptor and a proposed docking pose of the GABARAP (1KOT model 15 dock 54a). The viewing direction is from the extracellular space towards the intracellular space. Only the intracellular helices of the GABA$_A$ receptor are shown in this diagram. GABARAP is shown in cyan, the intracellular helix of the γ_2-subunit in red, that of the α_1-subunit in yellow and the helix of the β_2-subunit is shown in green

FIGURE 2 Side-view of a model of the GABA$_A$ receptor and a proposed docking pose of the GABARAP (1KOT model 15 dock 54a). Only the intracellular helices of the GABA$_A$ receptor is shown in this diagram. GABARAP is shown in cyan, the intracellular helix of the γ_2-subunit in red, that of the α_1-subunit in yellow and the helix of the β_2-subunit is shown in green

lengthened to 2 fs over 30 000 time-steps, during which period all main-chain nitrogen atoms of the three helices were tethered with a force constant of 2 kJ/mol/Å^2. These helices are part of a large protein and the helical structures are stabilized by neighboring structures, some of unknown configuration. In this study, we included only the helices and so to stabilize them, we imposed the tethers. A 50-ns equilibration was carried out on the initialized system, followed by a data collection period of 100 ns. Equilibration was confirmed by a stable r.m.s. deviation from the starting structure and, in the case of the pentahelix/GABARAP complex, a stable intermolecular distance. Configurations were output every 20 ps. A convex hull was created using the following 10 amino acids as vertices (they are at the end points of the five intracellular helices) using a previously developed method[19]: chain A (β_2-subunit) His 421 and Asp 450, chain B (γ_2-subunit) Asp 413 and Asp 442, chain C (α_1-subunit) Lys 391 and Asp 420, chain D (β_2-subunit) His 421 and Asp 450 and chain E (α_1-subunit) Lys 391 and Asp 420. These 10 amino acids are shown in Figure 3; the vertices on the membrane side lie (upper side of the diagram) in the plane where $z \sim 20$ Å and those on the intracellular side (lower side of the diagram) lie in the plane where $z \sim -20$ Å. The number of Cl^- ions inside this convex hull was determined using a previously developed method[20] and counted for every configuration.

We tracked the trajectories of the ions to locate movements which are similar to Cl^- ion movements when the GABA$_A$ receptor is conducting naturally. We define a "natural" ion movement where the Cl^- ion moves into the convex hull from the membrane side across the plane where $z \sim 20$ Å and where it exits from one of the five side portals at positions where $z < 15$ Å (see Figure 3); previous experiments show that these side portals are the exit routes for ions.[21]
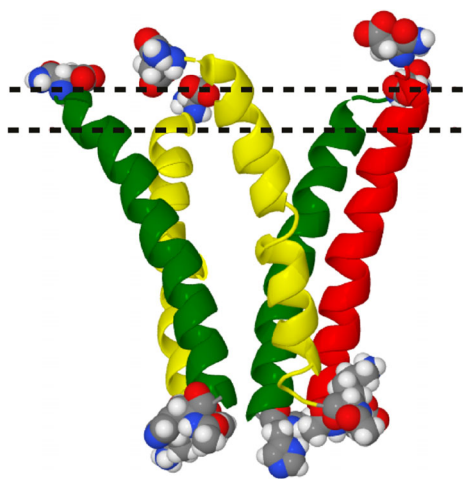

FIGURE 3 Side-view of a model of the GABA$_A$ receptor intracellular domain; the amino acids which form the vertices of the convex hull are shown in CPK models. The intracellular helix of the γ_2-subunit is shown in red, that of the α_1-subunit in yellow and that of the β_2-subunit is shown in green. The top dashed line is where $z = 20$ Å and the bottom dashed line is where $z = 15$ Å

2.3 | Evaluation of electrostatic potential

We calculated the electrostatic potential around the GABA$_A$ receptor intracellular pentahelix, in the absence and presence of GABARAP. From the 100-ns data production run of the molecular dynamics simulation, we took a configuration at every 10 ns to obtain 10 configurations. The water molecules and ions were removed from these configuration and, for each configuration, we calculated the electrostatic potential due to the CHARMM partial charges[18] on the protein atoms using simple Coulombic interactions; the dielectric constant was taken as one and nonperiodic boundary conditions were applied. We then averaged the potential over the 10 configurations and compared them in the absence and presence of GABARAP.

3 | RESULTS

3.1 | Molecular dynamics simulations

The GABA$_A$ receptor intracellular pentahelix atoms moved little during the course of the 100 ns data collection simulation, as they were tethered. GABARAP was not tethered, but it stayed in close proximity of the pentahelix. The volume enclosed by the amino acids at the end points of the intracellular helices were calculated using a previously developed method[22] and it remained stable at a value of about 27 nm^3 during the course of the simulation (data not shown). We measured the distances between, respectively, GABARAP Lys 46 Nζ and the GABA$_A$ receptor γ-subunit Asp 423 main-chain O, and GABARAP Gln 59 Cγ and the GABA$_A$ receptor γ-subunit Ile 438 Cδ and used these distances as indicators of the distance between these two proteins. The results are shown in Figure 4. It can be seen that the distances are relatively constant, which shows that the complex was stable throughout the data collection period.

Figure 5 shows the number of ions inside the convex hull enclosed by the pentahelix. There is an average of 2.8 Cl^- ions inside the convex hull in the absence of GABARAP, but on GABARAP binding this increases to 4.0 Cl^- ions. The number of ions in the pentahelix changes over time as the ions move in and out of the pentahelix, which is a pre-requisite for conduction. Moreover, in the presence of GABARAP, the average number of ions in the pentahelix is about 40% higher than in the absence of GABARAP, suggesting that more ions may be moving through the channel. In the absence of GABARAP, there are configurations when the channel has no ions, at which point it cannot be conducting ions.

We observed ions moving from the membrane side of the convex hull, through the hull of the pentahelix, then exiting from one of the five portals on the side, at positions where $z < 15$ Å. Figure 6 shows examples of such movements. Note that these ion passage trajectories usually last <1 ns, and they are short events on the timescale of the simulation. We observed 32 such events when GABARAP was absent but 60 such events when GABARAP was present during the 100 ns molecular dynamics simulations.
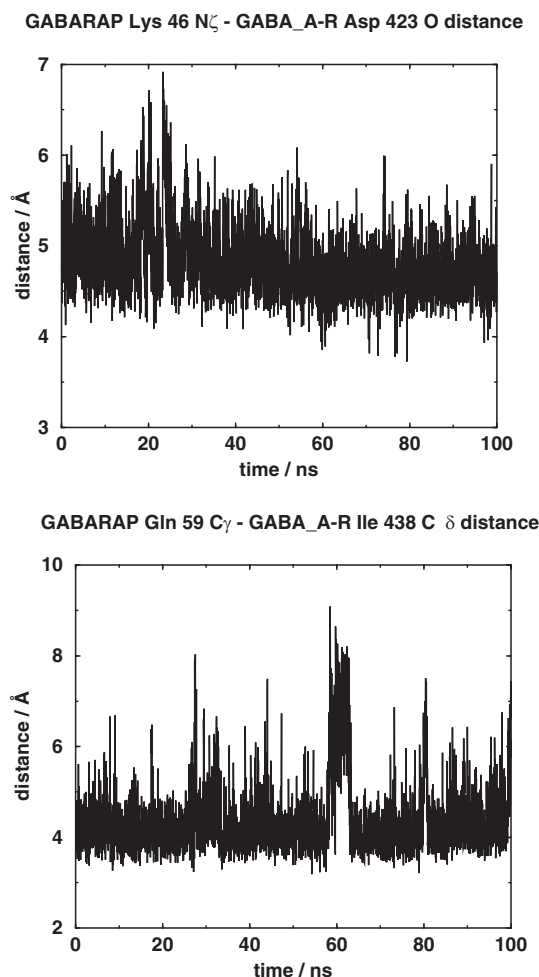
GABARAP Lys 46 Nζ - GABA_A-R Asp 423 O distance

GABARAP Gln 59 Cγ - GABA_A-R Ile 438 C δ distance

FIGURE 4 The upper panel shows the distance between the GABARAP Lys 46 Nζ atom and the GABA$_A$ receptor γ-subunit Asp 423 main-chain oxygen atom and the lower panel shows the distance between the GABARAP Gln 59 Cγ atom and the GABA$_A$ receptor γ-subunit Ile 438 Cδ atom

3.2 | Electrostatic potential

We visualize the electrostatic potentials due to the protein(s) by displaying the values on different planes using a color-coded scheme. In Figure 7, the electrostatic potential is displayed on a plane perpendicular to the central axis of the receptor. In the absence of GABARAP, the electrostatic potential is more positive in the region around the β_2-subunits. In the presence of GABARAP, there is a finger-like "extension" of more positive electrostatic potential through the slit made by the β_2- and γ_2-subunits next to the bound GABARAP. The region over which the electrostatic potential increases is largely outside the pentahelix.

In Figures 8 and 9, the electrostatic potential is displayed on five planes through each of the five slits formed by the GABA$_A$ receptor intracellular helices. In Figure 8, the electrostatic potential due to the intracellular helices alone is displayed. In Figure 9, the electrostatic potential due to the intracellular helices and GABARAP is shown. It can be seen that the effect of GABARAP on the electrostatic potential
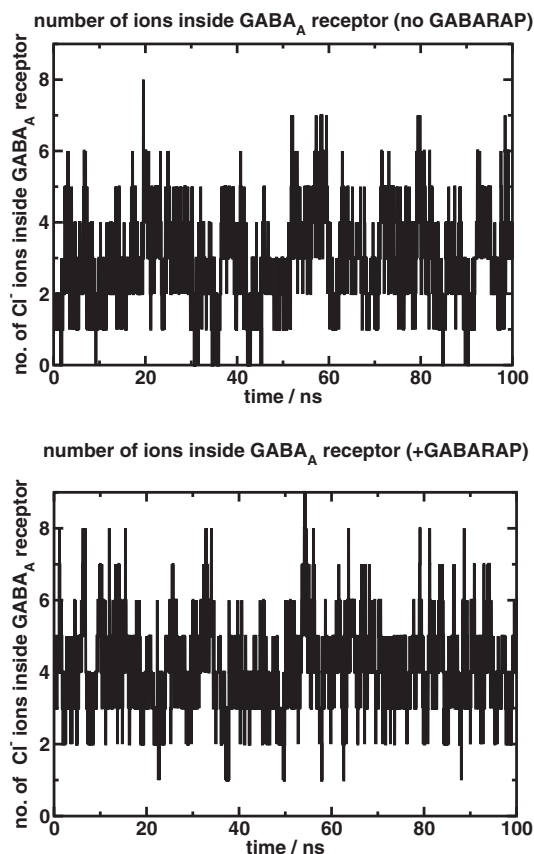
number of ions inside GABA$_A$ receptor (no GABARAP)

number of ions inside GABA$_A$ receptor (+GABARAP)

FIGURE 5 Number of ions inside the convex hull in the absence of GABARAP (upper panel) and in the presence of GABARAP (lower pane)

in planes (B) and (C) is small. However, in planes (A), (D) and (E), the electrostatic potential is more positive in the region outside the intracellular helices (Figure 9). To make it easier to visualize these changes in electrostatic potential, we plot the difference potential in Figure 10; this is the difference in electrostatic potential between the case where GABARAP is absent and the case where GABARAP is present. A positive difference means that the electrostatic potential in the presence of GABARAP is more positive than in its absence. It can be seen from Figure 10 that most regions outside the pentahelix become electrostatically more positive due to the presence of GABARAP, but some regions towards the cytoplasmic end inside the pentahelix become more negative. We suggest that this increase in electrostatic potential outside the receptor with a concomitant decrease in potential inside the receptor leads to the increase in Cl$^-$ ion conductance.

4 | DISCUSSION

Cys-loop ligand-gated ion channels often interact with cytoplasmic proteins, and this interaction serves many purposes, amongst them the clustering of ion channels and the modulation of channel function.
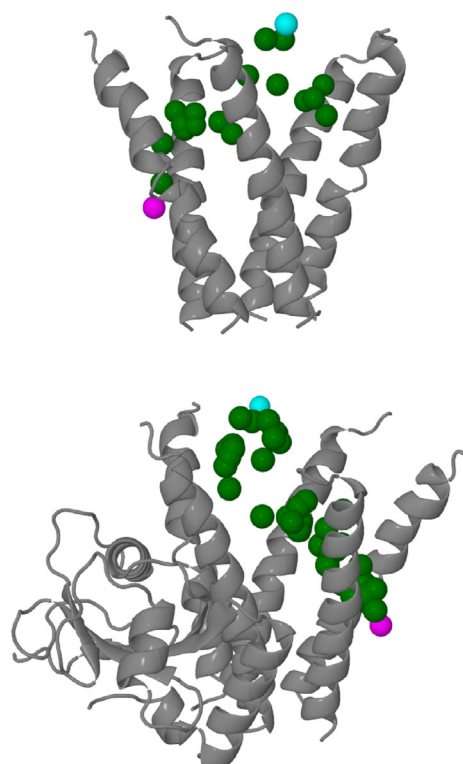
FIGURE 6 The top diagram shows a Cl⁻ ion entering the convex hull from the membrane side and exiting it from one of the five portals on the side at a level where $z = -4.4$ Å. The protein is shown in grey, the Cl⁻ ions in green except for the starting position (in cyan) and the finishing position (in magenta). Each position of the Cl⁻ ion is 20 ps apart. The bottom diagram shows a similar event but in the presence of GABARAP. Both trajectories are under 1 ns
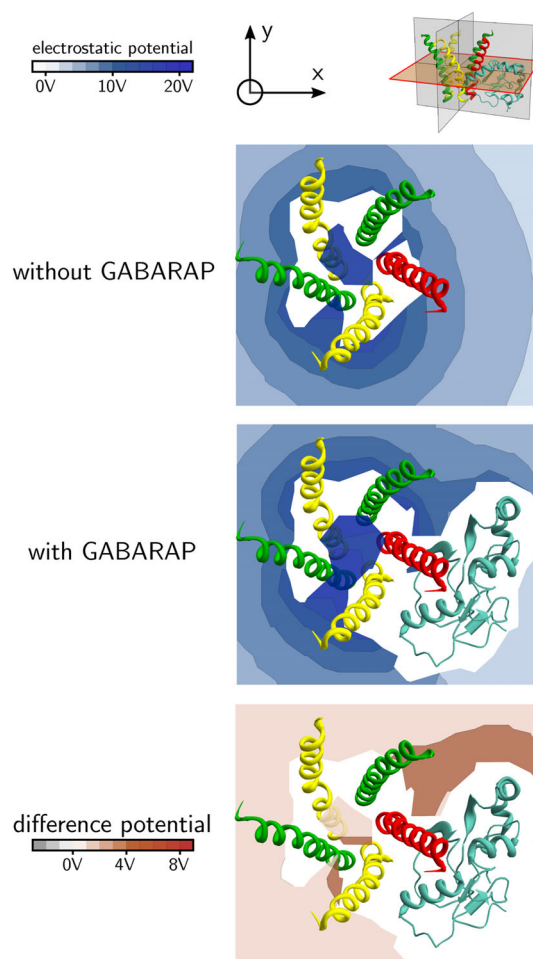

FIGURE 7 Electrostatic potential around GABAₐ receptor intracellular helices. The top panel shows, respectively from left to right, the electrostatic potential scale, the axes of the system and a diagram showing the transverse plane. The second panel shows the electrostatic potential on the plane in the absence of GABARAP, and the third panel shows the potential in the presence of GABARAP. The bottom panel shows the difference in electrostatic potential between the two cases. The α_1-subunit is shown in yellow, the β_2-subunit is shown in green and the γ_2-subunit is shown in red

For example, the muscle nicotinic acetylcholine receptor (nAChR) interacts with the cytoplasmic protein rapsyn. Rapsyn has a molecular weight of about 43 000,[23] and electron microscopy showed that the nAChR are interconnected by rapsyn dimers. Up to three rapsyn dimers can contact each nAChR in specific regions in the nAChR intracellular domain.[24] This tight network probably anchors the nAChR in the plane of the cell membrane and allows nAChR to be concentrated at the neuromuscular junction motor end-plate.[24]

Another example is gephyrin. This protein was first identified as a bridge between the glycine receptor and tubulin.[25] Sola et al.[26] co-crystallized a segment of the glycine receptor β-subunit and a partial dimer of the cytoplasmic protein gephyrin (Protein Data Bank code: 1T3E). They resolved the structure of a pentapeptide portion of the glycine receptor β-subunit and the gephyrin domain E dimer. These scientists proposed a network of gephyrin molecules linking the glycine receptors.

Gephyrin also interacts with the GABAₐ receptor through the receptor α_2-subunit[27] and α_3-subunit.[28] It is unclear if gephyrin binds the α_1-subunit of the GABAₐ receptor; some experiments failed to show any interaction,[29] but others showed a weak interaction.[30] Maric et al.[31] co-crystallized segments of the α_3-subunit of the GABAₐ receptor with segments of gephyrin, and identified the

undecapeptide T^{367}FNIVGTTYPIN^{381} from the GABAₐ receptor as important for interaction with gephyrin. They showed that there were similarities between the binding of the GABAₐ receptor and of the glycine receptor to gephyrin: in particular, T^{367}FNIVGTT^{374} from the GABAₐ receptor, and F^{398}SIVGSL^{404} from the glycine receptor β-subunit adopted similar conformations.

In addition to gephyrin, the GABAₐ receptor also interacts with collybistin; there are two types of collybistin, which consist of 413 and 493 amino acids, respectively.[32] Saiepour et al.[29] showed that collybistin interacted with the intracellular domain of the α_2-subunit of the GABAₐ receptor, and its binding site for the α_2-subunit overlapped that for gephyrin. Collybistin was later shown to be important for clustering gephyrin and the GABAₐ receptor.[33]

The GABAₐ receptor also interacts with GABARAP. GABARAP binds specifically to the γ_2-subunit of the GABAₐ receptor. Binding of
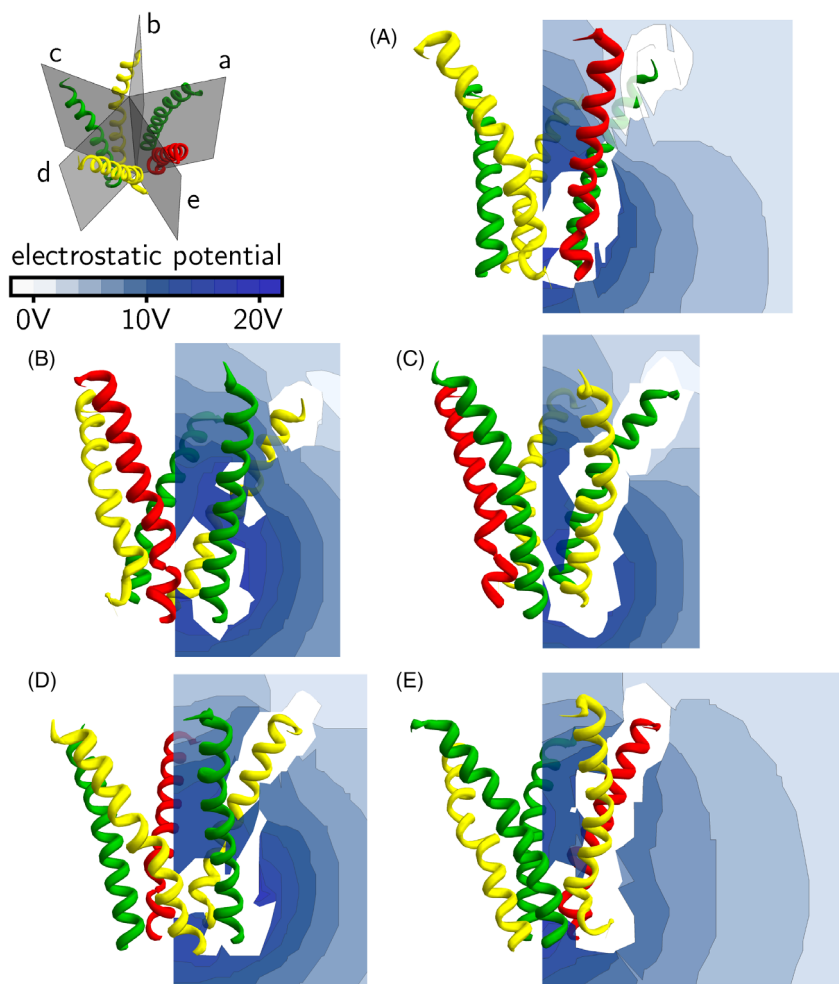
GABARAP to the GABA$_A$ receptor causes receptor clustering,[10,34] so some of its functions are similar to gephyrin and collybistin. However, GABARAP is unique in that its binding also causes the conductance of the GABA$_A$ receptor to increase from about 30 pS to 40 pS–60 pS, and the mean channel opening times from about 2 ms to about 6 ms.[11] It thus appears that gephyrin has more general actions on both the GABA$_A$ receptor and the glycine receptor, and that the action of gephyrin and collybistin appear to be confined to receptor clustering. The action of GABARAP is more specific to the GABA$_A$ receptor, and, in addition to receptor positioning, it also modulates the electrophysiology of this ion channel.

The GABA$_A$ receptors in neurons have different ion channel properties from recombinant receptors.[35] Luu et al.[11] show that GABA$_A$ receptor conductances in neurons is similar to that obtained from recombinant receptors associated with GABARAP. GABARAP is thus of importance in physiological functioning of the GABA$_A$ receptor in the central nervous system, and this underlies the importance of understanding the physiological role of the intracellular domain of this receptor.

In this study, we used a simplified system of a modeled GABA$_A$ receptor consisting only of its intracellular domain and studied its electrostatic properties in the absence and presence of GABARAP.

Our results show that GABARAP increases the electrostatic potential of the region around and outside the intracellular domain; this is consistent with increased Cl$^-$ conductance. Our results also show that the number of ions in the pentahelix varies significantly in time as they move in and out of the pentahelix, which is a pre-requisite for conduction. Moreover, in the presence of GABARAP, the average number of ions in the pentahelix is more than 40% higher, suggesting that more ions may be moving through the channel. In the absence of GABARAP, there are configurations when the channel has no ions, at which point it cannot be conducting ions. Further analysis shows that ion movements through the convex hull of the pentahelix similar to "natural" conducting currents are almost twice as frequently observed in the presence of GABARAP. In both cases the number of these conduction events observed during a 100-ns period was over 10 times higher than the average number of ions in the convex hull, and there was no evidence of a long-term increase or reduction in the number of ions inside the hull.

Previous experimental results[11,35] and our findings in this article show that GABARAP binding to the GABA$_A$ receptor increases the receptor channel conductance. However, the exact role of GABARAP is thrown into doubt by recent experiments. Everitt et al.[34] suggest that GABARAP is not involved in altering GABA$_A$ receptor

FIGURE 9 Electrostatic potential around GABA_A receptor intracellular helices and GABARAP. The α_1-subunit is shown in yellow, the β_2-subunit is shown in green, the γ_2-subunit is shown in red and GABARAP shown in cyan. The top left panel shows five planes, each cutting through one of the five slits formed by the helices. The electrostatic potential due to the proteins is calculated and displayed in a color-coded scheme. Panels (A–E) show the electrostatic potential on the same five planes as in Figure 8
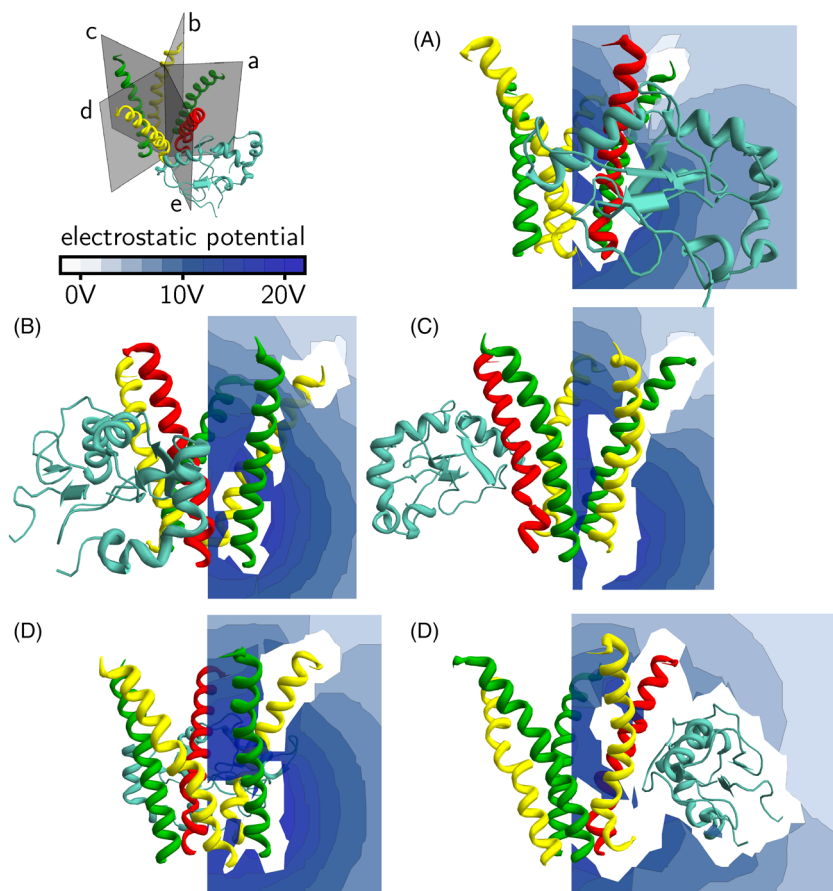

FIGURE 10 Difference electrostatic potential (the difference in electrostatic potential between the case where GABARAP is absent and the case where GABARAP is present) around GABA_A receptor intracellular helices. The α_1-subunit is shown in yellow, the β_2-subunit is shown in green, the γ_2-subunit is shown in red and GABARAP shown in cyan. The top left panel shows five planes, each cutting through one of the five slits formed by the helices. The difference electrostatic potential due to the protein alone is calculated and displayed in a color-coded scheme; a positive difference means that the electrostatic potential in the presence of GABARAP is more positive than in its absence. Panels (A–E) show the difference electrostatic potential on the same five planes as in Figure 8
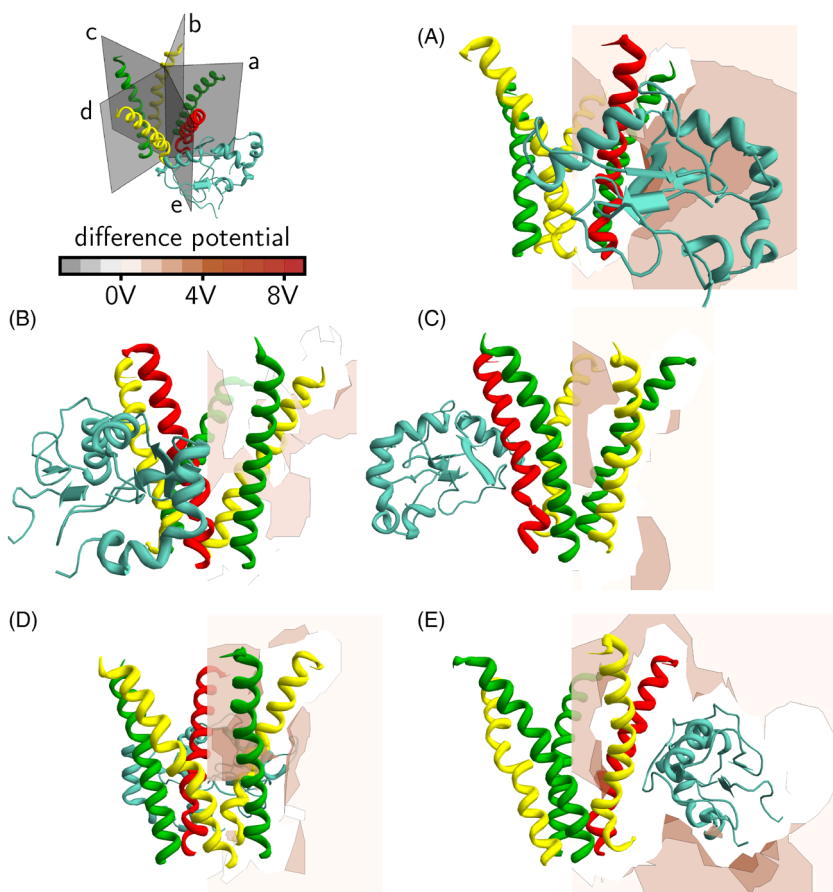
conductance. Tierney[36] suggests that adjacent $GABA_A$ receptors interact via their solitary γ_2-subunit MA helices; the ionic conductance is thus increased by this interaction. However, in the suggested mechanism, the γ_2-subunit of one $GABA_A$ receptor swings out to interact with the γ_2-subunit of another receptor, which involves a large structural change. These results seem to contradict previous experimental findings.[11,35]

To define the interaction between GABARAP and the $GABA_A$ receptor in greater detail and to understand how GABARAP changes the receptor structure and function would require high-resolution structures of the $GABA_A$ receptor with an intact intracellular domain, in the absence and presence of GABARAP. This should then be accompanied by electrophysiology experiments where, ideally, the behavior of three membrane patches are compared: the first patch contains one single active $GABA_A$ receptor and no GABARAP, the second patch contains one single active $GABA_A$ receptor with GABARAP, and the third patch contains two or more active $GABA_A$ receptors. In the third patch, the interaction between the individual $GABA_A$ receptors can be disrupted using different peptides to define the interaction between the different molecules. This kind of system would allow us to examine in detail the apparent contradiction in previous experimental results[11,34–36] and arrive at a better understanding of the function of GABARAP.

CONFLICT OF INTEREST

The authors declare no conflict of interest.

PEER REVIEW

The peer review history for this article is available at https://publons.com/publon/10.1002/prot.26241.

DATA AVAILABILITY STATEMENT

"The simulation data are available on request from the corresponding author (pc104@pasteur.fr) but in due course they will be put on a server where they can be downloaded by readers."

ORCID

P.-L. Chau https://orcid.org/0000-0003-3614-1561

REFERENCES

1. Nayeem N, Green TP, Martin IL, Barnard EA. Quaternary structure of the native $GABA_A$ receptor determined by electron microscopic image analysis. *J Neurochem*. 1994;62:815-818.
2. Sigel E, Steinmann ME. Structure, function, and modulation of $GABA_A$ receptors. *J Biol Chem*. 2012;287:40224-40231.
3. Whiting PJ. GABA-A receptor subtypes in the brain: a paradigm for CNS drug discovery? *Drug Discov Today*. 2003;8:445-450.
4. Farrar SJ, Whiting PJ, Bonnert TP, McKernan RM. Stoichiometry of a ligand-gated ion channel determined by fluorescence energy transfer. *J Biol Chem*. 1999;274:10100-10104.
5. Nistri A, Constanti A. Pharmacological characterization of different types of GABA and glutamate receptors in vertebrates and invertebrates. *Prog Neurobiol*. 1979;13:117-235.
6. Mathers DA. The $GABA_A$ receptor: new insights from single-channel recording. *Synapse*. 1987;1:96-101.
7. Wang H, Bedford FK, Brandon NJ, Moss SJ, Olsen RW. $GABA_A$-receptor-associated protein links $GABA_A$ receptors and the cytoskeleton. *Nature*. 1999;397:69-72.
8. Nymann-Andersen J, Wang H, Chen L, Kittler JT, Moss SJ, Olsen RW. Subunit specificity and interaction domain between $GABA_A$ receptor-associated protein (GABARAP) and $GABA_A$ receptors. *J Neurochem*. 2002;80:815-823.
9. Coyle JE, Qamar S, Rajashankar KR, Nikolov DB. Structure of GABARAP in two conformations: implications for $GABA_A$ receptor localization and tubulin binding. *Neuron*. 2002;33:63-74.
10. Chen L, Wang H, Vicini S, Olsen RW. The γ-aminobutyric acid type A ($GABA_A$) receptor-associated protein (GABARAP) promotes $GABA_A$ receptor clustering and modulates the channel kinetics. *Proc Natl Acad Sci USA*. 2000;97:11557-11562.
11. Luu T, Gage PW, Tierney ML. GABA increases both the conductance and mean open time of recombinant $GABA_A$ channels co-expressed with GABARAP. *J Biol Chem*. 2006;281:35699-35708.
12. Irwin BWJ, Vukovič S, Payne MC, ElGamacy M, Chau P-L. Prediction of GABARAP interaction with the GABA type A receptor. *Proteins*. 2018;86:1251-1264.
13. Mokrab Y, Bavro VN, Mizuguchi K, et al. Exploring ligand recognition and ion flow in comparative models of the human GABA type A receptor. *J Mol Graph Model*. 2007;26:760-774.
14. Unwin N. Refined structure of the nicotinic acetylcholine receptor at 4 Å resolution. *J Mol Biol*. 2005;346:967-989.
15. Stangler T, Mayr LM, Willbold D. Solution structure of human $GABA_A$ receptor-associated protein GABARAP. *J Biol Chem*. 2002;277:13363-13366.
16. Jo S, Kim T, Iyer VG, Im W. Software news and updates: CHARMM-GUI—a web-based graphical user interface for CHARMM. *J Comput Chem*. 2008;29:1859-1865.
17. Phillips JC, Braun R, Wang W, et al. Scalable molecular dynamics with NAMD. *J Comput Chem*. 2005;26:1781-1802.
18. MacKerell AD, Bashford D, Bellott M, et al. All-atom empirical potential for molecular modeling and dynamics studies of proteins. *J Phys Chem B*. 1998;102:3586-3616.
19. Clarkson KL, Mehlhorn K, Seidel R. Four results on randomized incremental constructions. *Comput Geomet*. 1993;3:185-212.
20. Chau P-L. Water movement during ligand unbinding from receptor site. *Biophys J*. 2004;87:121-128.
21. Hales TG, Dunlop JI, Deeb TZ, et al. Common determinants of single channel conductance within the large cytoplasmic loop of 5-hydroxytryptamine type 3 and $\alpha_4\beta_2$ nicotinic acetylcholine receptors. *J Biol Chem*. 2006;281:8062-8071.
22. Chan SL, Purisima EO. Molecular surface generation using marching tetrahedra. *J Comput Chem*. 1998;19:1268-1277.
23. Ramarao MK, Bianchetta MJ, Lanken J, Cohen JB. Role of rapsyn tetratricopeptide repeat and coiled-coil domains in self-association

and nicotinic acetylcholine receptor clustering. *J Biol Chem*. 2001; 276:7475-7483.

24. Zuber B, Unwin N. Structure and superorganization of acetylcholine receptor-rapsyn complexes. *Proc Natl Acad Sci USA*. 2013;110: 10622-10627.

25. Kirsch J, Langosch D, Prior P, Littauer UZ, Schmitt B, Betz H. The 93-kDa glycine receptor-associated protein binds to tubulin. *J Biol Chem*. 1991;266:22242-22245.

26. Sola M, Bavro VN, Timmins J, et al. Structural basis of dynamic glycine receptor clustering by gephyrin. *EMBO J*. 2004;23:2510-2519.

27. Tretter V, Jacob TC, Mukherjee J, Fritschy J-M, Pangalos MN, Moss SJ. The clustering of GABA$_A$ receptor subtypes at inhibitory synapses is facilitated via the direct binding of receptor α_2 subunits to gephyrin. *J Neurosci*. 2008;28:1356-1365.

28. Tretter V, Kerschner B, Milenkovic I, et al. Molecular basis of the γ-aminobutyric acid A receptor α_3 subunit interaction with the clustering protein gephyrin. *J Biol Chem*. 2011;286:37702-37711.

29. Saiepour L, Fuchs C, Patrizi A, Sassoe-Pognetto M, Harvey RJ, Harvey K. Complex role of collybistin and gephyrin in GABA$_A$ receptor clustering. *J Biol Chem*. 2010;285:29623-29631.

30. Mukherjee J, Kretschmannova K, Gouzer G, et al. The residence time of GABA$_A$Rs at inhibitory synapses is determined by direct binding of the receptor α_1 subunit to gephyrin. *J Neurosci*. 2011;31:14677-14687.

31. Maric HM, Kasaragod VB, Hausrat TJ, et al. Molecular basis of the alternative recruitment of GABA$_A$ versus glycine receptors through gephyrin. *Nat Commun*. 2014;5:5767.

32. Kins S, Betz H, Kirsch J. Collybistin, a newly identified brain-specific GEF, induces submembrane clustering of gephyrin. *Nat Neurosci*. 2000;3:22-29.

33. Chiou T-T, Bonhomme B, Jin H, et al. De. Differential regulation of the postsynaptic clustering of γ-aminobutyric acid type A (GABA$_A$) receptors by collybistin isoforms. *J Biol Chem*. 2011;286:22456-22468.

34. Everitt AB, Seymour VAL, Curmi J, Laver DR, Gage PW, Tierney ML. Protein interactions involving the γ_2 large cytoplasmic loop of GABA$_A$ receptors modulate conductance. *FASEB J*. 2009;23:4361-4369.

35. Everitt AB, Luu T, Cromer B, et al. Conductance of recombinant GABA$_A$ channels is increased in cells co-expressing GABA$_A$ receptor-associated protein. *J Biol Chem*. 2004;279:21701-21706.

36. Tierney ML. Insights into the biophysical properties of GABA$_A$ ion channels: modulation of ion permeation by drugs and protein interactions. *Biochim Biophys Acta*. 2011;1808:667-673.